

Highly Luminescent Gold(I)–Silver(I) and Gold(I)–Copper(I) Chalcogenide Clusters

Olga Crespo, M. Concepción Gimeno,* Antonio Laguna, Carmen Larraz, and M. Dolores Villacampa^[a]

Abstract: The reactions of $[\text{AuClL}]$ with Ag_2O , where L represents the heterofunctional ligands PPh_2py and $\text{PPh}_2\text{CH}_2\text{CH}_2\text{py}$, give the trigoldoxonium complexes $[\text{O}(\text{AuL})_3]\text{BF}_4$. Treatment of these compounds with thio- or selenourea affords the triply bridging sulfide or selenide derivatives $[\text{E}(\text{AuL})_3]\text{BF}_4$ ($\text{E}=\text{S}, \text{Se}$). These trinuclear species react with $\text{Ag}(\text{OTf})$ or $[\text{Cu}(\text{NCMe})_4]\text{PF}_6$ to give different results, depending on the phosphine and the metal. The reactions of $[\text{E}(\text{AuPPh}_2\text{py})_3]\text{BF}_4$ with silver or copper salts give $[\text{E}(\text{AuPPh}_2\text{py})_3\text{M}]^{2+}$ ($\text{E}=\text{O}$,

$\text{S}, \text{Se}; \text{M}=\text{Ag}, \text{Cu}$) clusters that are highly luminescent. The silver complexes consist of tetrahedral Au_3Ag clusters further bonded to another unit through aurophilic interactions, whereas in the copper species two coordination isomers with different metallophilic interactions were found. The first is analogous to the silver complexes and in the second, two $[\text{S}(\text{AuPPh}_2\text{py})_3]^+$

units bridge two copper atoms through one pyridine group in each unit. The reactions of $[\text{E}(\text{AuPPh}_2\text{CH}_2\text{CH}_2\text{py})_3]\text{BF}_4$ with silver and copper salts give complexes with $[\text{E}(\text{AuPPh}_2\text{CH}_2\text{CH}_2\text{py})_3\text{M}]^{2+}$ stoichiometry ($\text{E}=\text{O}, \text{S}, \text{Se}; \text{M}=\text{Ag}, \text{Cu}$) with the metal bonded to the three nitrogen atoms in the absence of $\text{Au}\cdots\text{M}$ interactions. The luminescence of these clusters has been studied by varying the chalcogenide, the heterofunctional ligand, and the metal.

Keywords: chalcogens • cluster compounds • copper • gold • luminescence • silver

Introduction

Luminescent d^{10} compounds have received increasing attention over past decades because of their interesting photophysical and photochemical properties and their possible applications in OLED display technology,^[1–3] as dopant emitters,^[4–8] and in sensors for luminescence-based detection of volatile organic compounds.^[9–12] Gold(I) complexes have received considerable attention recently because they exhibit unique features, such as the formation of secondary bonds through aurophilic interactions^[13,14] that are similar in strength to hydrogen bonds. These attractions between closed-shell atoms result from electronic correlation effects strengthened by the large relativistic effects of gold.^[15] Gold

also forms many metallophilic $\text{Au}\cdots\text{M}$ interactions which are of great interest because of their influence on molecular structure and physical properties, such as luminescence.

We are interested in the chemistry of chalcogenide gold compounds; several reports have dealt with this type of compound^[14,16–18] and they have been shown to have luminescence properties.^[18] We have shown that chalcogenides can bind from two to six gold atoms, forming electron-deficient complexes of the type $[\text{E}(\text{AuPPh}_3)_n]^{(n-2)+}$ ($n=4, 5, 6$).^[16] We have also reported on chalcogenide-centered complexes with gold atoms in different oxidation states,^[17] but all attempts to prepare heteronuclear derivatives have led to a mixture of complexes. As far as we are aware only the mixed-metal chalcogenide-centered complexes $[(\text{O}(\text{AuPPh}_3)_2(\text{Rh}\{\text{dien}\}))_2](\text{BF}_4)_2$ ($\text{dien}=1,5\text{-cyclooctadiene (cod), norbornadiene (nbd)}$),^[19] $[(\text{O}(\text{AuPPh}_3)(\text{Pt}\{\text{cod}\}))_2](\text{BF}_4)_2$,^[20] $[(\text{O}(\text{AuPPh}_3)\text{Pd}(t\text{Bu}_2\text{bipy}))_2]^{2+}$,^[21] $[(\text{S}(\text{AuPPh}_3)_3)_2\text{Ag}(\text{thf})](\text{BF}_4)_3$,^[22] $[\text{Au}_4(\text{SeInCl}_3)_2\text{Ph}_2\text{P}(\text{CH}_2)_5\text{PPh}_2]_2$,^[23] and $[\text{Au}_8\text{Se}_4\text{In}(\text{Ph}_2\text{P}(\text{CH}_2)_2\text{PPh}_2]_4](\text{InCl}_4)_3$,^[23] have been reported. A strategy to prepare these chalcogenide-centered heteronuclear derivatives involves the use of heterofunctional ligands such as the phosphines PPh_2py or $\text{PPh}_2\text{CH}_2\text{CH}_2\text{py}$. We have chosen both ligands because of their different capabili-

[a] O. Crespo, Prof. M. C. Gimeno, Prof. A. Laguna, C. Larraz, M. D. Villacampa
Departamento de Química Inorgánica
Instituto de Ciencia de Materiales de Aragón
Universidad de Zaragoza-CSIC, 50009 Zaragoza (Spain)
Fax: (+34) 976-761-187
E-mail: gimeno@unizar.es

 Supporting information for this article is available on the WWW under <http://www.chemeurj.org> or from the author.

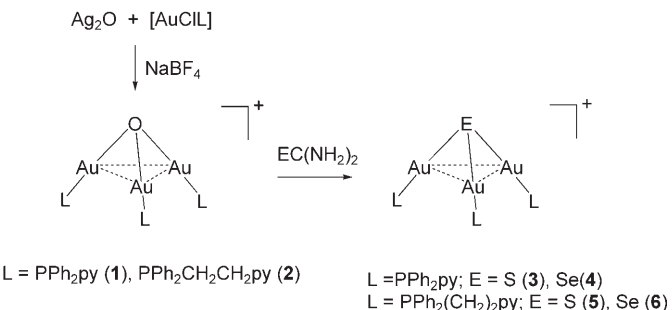
ties in promoting the Au···M interaction, since they would form five- and seven-membered metallacycles, respectively. We have previously communicated the synthesis of $[E(AuPPh_2py)_3Ag]^{2+}$ ($E=O, S, Se$) complexes, which have a tetrahedral Au_3Ag skeleton with short Au···Ag interactions.^[24] These complexes are highly luminescent and their emissions move from the blue to the green to the orange region on going from oxygen to sulfur to selenium. Herein we report on the reactivity of $[E(AuL)]^+$ complexes, where L represents the heterofunctional ligand and E the chalcogenide, with silver and copper compounds. A study of their luminescence with variation of the chalcogenide, the heterofunctional ligand, and the metal has been carried out. The chalcogenide ligand influences the emission energies, the heterofunctional ligand the formation of metallophilic interactions, and the metal is important in determining the strength of the Au···M interactions which are key to the luminescent properties.

Results and Discussion

The reactions of $[AuCl(PPh_2py)]$ or $[AuCl(PPh_2CH_2CH_2py)]$ with Ag_2O in the presence of $NaBF_4$ gave the oxonium derivatives $[O(AuPPh_2py)_3]BF_4$ (**1**) and $[O(AuPPh_2CH_2CH_2py)_3]BF_4$

Abstract in Spanish: La reacción de los complejos $[AuClL]$ con Ag_2O , donde L representa un ligando heterodifuncional como PPh_2py y $PPh_2CH_2CH_2py$, da lugar a los derivados tri-nucleares de oxonio, $[O(AuL)_3]BF_4$. El tratamiento de estos compuestos con tiourea o selenourea conduce a la obtención de las especies con los átomos de azufre o selenio puente a tres centros metálicos, $[E(AuL)_3]BF_4$ ($E=S, Se$). Estas especies tri-nucleares reaccionan posteriormente con $Ag(OTf)$ o $[Cu(NCMe)_4]PF_6$ con diferentes resultados, dependiendo del ligando fosfina y del metal. La reacción de $[E(AuPPh_2py)_3]BF_4$ con compuestos de plata o cobre da lugar a los clusters $[E(AuPPh_2py)_3M]^{2+}$ ($E=O, S, Se; M=Ag, Cu$) que presentan una intensa luminiscencia. La estructura para los complejos de plata consiste en dos unidades tetraédricas Au_3Ag que se asocian a través de interacciones aurofilicas, mientras que para los derivados de cobre se observan dos isómeros de coordinación con diferentes interacciones metalófilicas. El primer isómero es análogo a los compuestos de plata y en el segundo dos unidades $[S(AuPPh_2py)_3]^+$ actúan como ligandos puente a los átomos de cobre a través de uno de los átomos de nitrógeno de una piridina. La reacción de $[E(AuPPh_2CH_2CH_2py)_3]BF_4$ con compuestos de plata o cobre conduce a derivados de estequiométrica $[E(AuPPh_2CH_2CH_2py)_3M]^{2+}$ ($E=O, S, Se; M=Ag, Cu$) donde el metal se coordina a los tres átomos de nitrógeno, sin que haya interacciones $Au\cdots M$. Se ha analizado la variación de las propiedades luminiscentes de estos sistemas al modificar diversos parámetros estructurales: el calcogenuro, el ligando heterodifuncional y el metal.

$py)_3]BF_4$ (**2**) in high yields. Both show a singlet in their $^{31}P\{^1H\}$ NMR spectra, at $\delta=23.4$ and 21.1 ppm, respectively, which are characteristic of oxonium tri(goldphosphine) complexes.^[25] Treatment of the oxonium compounds with thiourea or selenourea gave the corresponding compounds with the sulfur or selenium atoms bridging the three gold atoms, $[E(AuPPh_2py)_3]BF_4$ ($E=S$ (**3**), Se (**4**)) or $[E(AuPPh_2CH_2CH_2py)_3]BF_4$ ($E=S$ (**5**), Se (**6**)), with urea as the by-product (see Scheme 1). Complexes **3–6** are white, air- and moisture-



Scheme 1.

stable solids that have been characterized by NMR and mass spectrometry. The $^{31}P\{^1H\}$ NMR spectra of **3–6** show only one resonance for the equivalent phosphorus atoms with chemical shifts ranging from $\delta=29.7$ to 33.6 ppm, quite different from those of the oxonium complexes.

X-ray crystal structure determinations were carried out on some of these complexes, namely $[O(AuPPh_2py)_3]PF_6$ (**1**), $[O(AuPPh_2CH_2CH_2py)_3]BF_4$ (**2**), and $[Se(AuPPh_2py)_3]BF_4$ (**4**). The cations of complexes **1** and **2** consist of Au_3O units that dimerize through aurophilic interactions (see the Supporting Information). The overall bonding scheme is typical of trigoldoxonium complexes.^[25,26] The structure of complex **4** is shown in Figure 1 and selected bond lengths and angles are listed in Table 1. The $Au\cdots Se$ distances are 2.4117(12)–2.4566(10) Å and are similar to those found in other μ_3 -Se

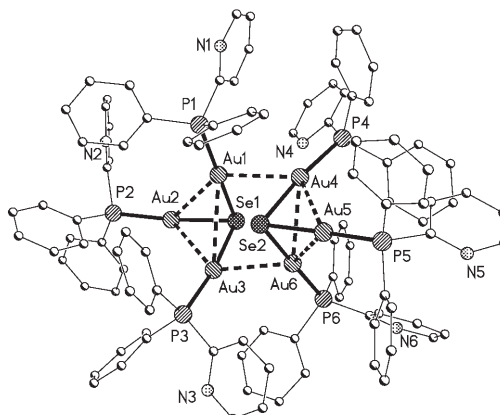


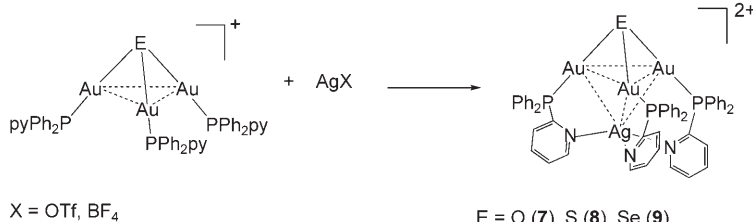
Figure 1. Structure of the cation of complex **4** with the atomic numbering scheme.

Table 1. Selected bond lengths [Å] and angles [°] for complex **4**.

Au1–P1	2.271(2)	Au3–Au6	2.9666(8)
Au1–Se1	2.4396(10)	Au4–P4	2.264(3)
Au1–Au4	3.1203(9)	Au4–Se2	2.4499(11)
Au1–Au2	3.1996(7)	Au4–Au6	3.0098(8)
Au1–Au3	3.3691(8)	Au4–Au5	3.1770(8)
Au2–P2	2.254(3)	Au5–P5	2.259(3)
Au2–Se1	2.4182(11)	Au5–Se2	2.4117(12)
Au2–Au6	3.0937(8)	Au5–Au6	3.2778(7)
Au3–P3	2.272(2)	Au6–P6	2.266(2)
Au3–Se1	2.4426(10)	Au6–Se2	2.4566(10)
P1–Au1–Se1	173.04(6)	Au2–Se1–Au1	82.39(3)
P2–Au2–Se1	173.30(7)	Au2–Se1–Au3	79.06(3)
P3–Au3–Se1	172.04(7)	Au1–Se1–Au3	87.27(3)
P4–Au4–Se2	171.49(7)	Au5–Se2–Au4	81.61(3)
P5–Au5–Se2	173.80(8)	Au5–Se2–Au6	84.64(4)
P6–Au6–Se2	175.82(7)	Au4–Se2–Au6	75.68(3)

gold complexes such as $[\text{Se}(\text{AuPPh}_3)_3]\text{PF}_6$.^[16d,27] The Au···Au interactions are in the range 2.9666(8)–3.3691(8) Å, which are longer than those in the corresponding oxonium salt, probably as a result of the larger size of the bridging chalcogenide.

The reactions of complexes **1**, **3**, or **4** with $\text{Ag}(\text{OTf})$ or AgBF_4 led to the previously reported^[24] gold(I)–silver(I) clusters $[\text{E}(\text{AuPPh}_2\text{py})_3\text{Ag}]^{2+}$ ($\text{E}=\text{O}$ (**7**), S (**8**), Se (**9**)) in which the heterofunctional ligand 2-diphenylphosphinopyridine, P-bonded to the gold(I) atoms, coordinates to the silver(I) atom through the nitrogen pyridine atom forming a tetrahedral Au_3Ag cluster (see Scheme 2). These complexes

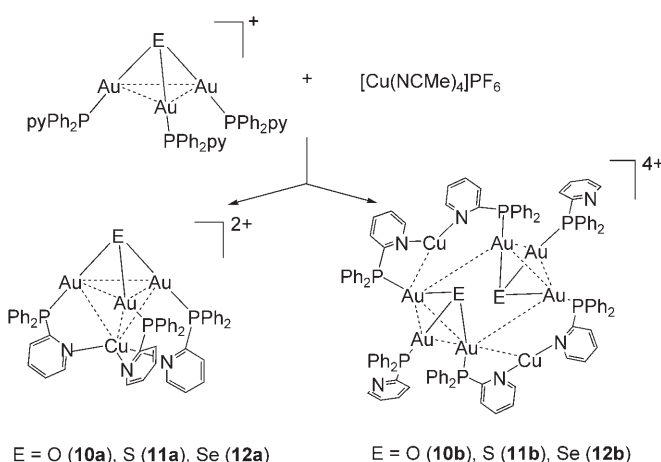


Scheme 2.

are brightly luminescent and exhibit a large variation in the emission maximum depending on the $\mu_3\text{-E}$ capping ligand, being blue for oxygen, green for sulfur, and orange for selenium.

As a consequence of the interesting luminescence properties of this type of complex we investigated the results of the reaction with other metal fragments such as copper(I). The reactions of $[\text{E}(\text{AuPPh}_2\text{py})_3]\text{BF}_4$ with $[\text{Cu}(\text{NCMe})_4]\text{PF}_6$ in dichloromethane led to the formation of complexes $[\text{E}(\text{AuPPh}_2\text{py})_3\text{Cu}](\text{BF}_4)(\text{PF}_6)$ ($\text{E}=\text{O}$ (**10**), S (**11**), Se (**12**)). These compounds are also intensely luminescent in the solid state. In the ${}^{31}\text{P}\{{}^1\text{H}\}$ NMR spectra two resonances are observed for complexes **10** and **12** (with an approximate ratio of 2:1) and a broad resonance for **11**. This is not consistent with the spectra recorded for the silver complexes **7**–**9** in which only one resonance was observed because of the

equivalence of the phosphorus atoms. Consequently, we carried out low-temperature NMR studies on complexes **10** and **12** which showed the presence of two major resonances in a ratio of 2:1 and three minor resonances. This data is consistent with the presence of a second species. In the case of complex **11** we can see a higher proportion of the second species. The compound that exhibits three singlets corresponds to a structure similar to the silver complexes in which the copper(I) atom binds to the three pyridine groups and also forms $\text{Au}(\text{I})\cdots\text{Cu}(\text{I})$ interactions (see Scheme 3).



Scheme 3.

Despite the equivalence of the phosphorus atoms in these complexes at room temperature up to three resonances are expected at low temperatures probably because of the differences in the $\text{Au}\cdots\text{Au}$ and $\text{Au}\cdots\text{Cu}$ interactions, as was previously observed in the spectra of gold complexes with a central sulfur or selenium atom.^[16b,d] The compounds with two main resonances correspond to a structure with inequivalent phosphorus atoms present in a ratio of 2:1. This is possible with a different coordination mode between the copper atom and the pyridine groups and, taking into account the high tendency of the starting materials to form dimers through aurophilic interactions, the metallic center could bind two pyridine groups from a different trinuclear unit (see Scheme 3). These two species are coordination isomers. The presence of these two isomers (**a** and **b**) has been confirmed by X-ray diffraction studies and both have been characterized for the sulfide compounds. For the sulfide complex **11** the ratio of the two isomers can be varied if the starting material is $[\text{S}(\text{AuPPh}_2\text{py})_3]\text{OTf}$ instead of $[\text{S}(\text{AuPPh}_2\text{py})_3]\text{BF}_4$, in which the trifluoromethanesulfonate anion, with a higher coordination capability, may bind to the copper atom thereby favoring isomer **b** (with a coor-

dinated OTf^- ion). Figure 2 shows a variable-temperature $^{31}\text{P}\{\text{H}\}$ NMR study of $[\text{S}(\text{AuPPPh}_2\text{py})_3\text{Cu}](\text{OTf})(\text{PF}_6)$ with the different intensities of the isomers. At room temperature

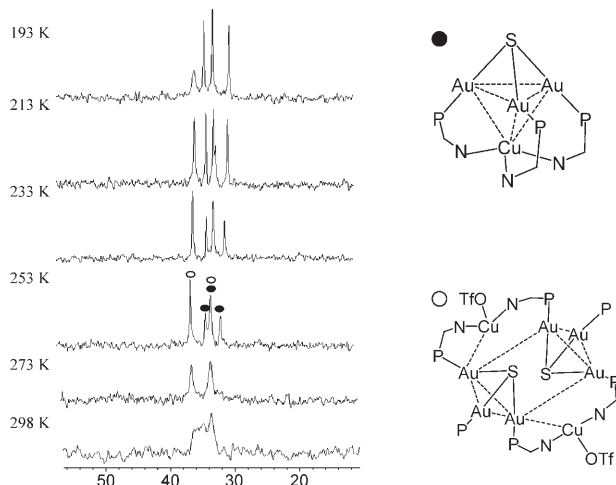


Figure 2. $^{31}\text{P}\{\text{H}\}$ NMR spectra of $[\text{S}(\text{AuPPPh}_2\text{py})_3\text{Cu}](\text{OTf})(\text{PF}_6)$ at different temperatures.

a broad resonance appears that splits into two at 273 K. At 253 K both isomers are observed, with isomer **a** exhibiting three singlets and isomer **b** two singlets. At 193 K the signals due to isomer **b** broaden and those due to isomer **a** seem to be present in a higher ratio, which suggests that the proportion of the two isomers is also temperature-dependent.

The question now is why only one type of structure has been detected in the silver(I) complexes, as indicated by their low-temperature $^{31}\text{P}\{\text{H}\}$ spectra in which three singlets due to three different phosphorus atoms are observed. Silver(I) and copper(I) are commonly found in a tetrahedral environment, but silver(I) is probably found more often in a trigonal planar geometry than copper(I), and many silver(I) complexes with the coordinated trifluoromethanesulfonate ligand have been described. A possible explanation for the presence of only one isomer in the silver complexes is that the $\text{Au}\cdots\text{Ag}$ interactions are stronger than $\text{Au}\cdots\text{Cu}$ interactions, leading to a greater stabilization of the Au_3Ag tetrahedral clusters relative to the Au_3Cu clusters.

The crystal structures of the two coordination isomers **11a** and **11b** were determined by X-ray diffraction studies. Crystals of **11a** were obtained from $[\text{S}(\text{AuPPPh}_2\text{py})_3\text{Cu}](\text{OTf})(\text{PF}_6)$ in dichloroethane/hexane, crystallizing as the dimer with three PF_6^- and one OTf^- ions, and crystals of **11b** were obtained from $[\text{S}(\text{AuPPPh}_2\text{py})_3\text{Cu}](\text{OTf})(\text{PF}_6)$ in dichloromethane/hexane. The cation of complex **11a** is shown in Figure 3 and selected bond lengths and angles are listed in Table 2. The asymmetric unit consists of two Au_3Cu monomers bonded through only one intermolecular $\text{Au}\cdots\text{Au}$ interaction of length 2.9496(6) Å in contrast to the structural unit observed in the starting material and also in the analogous silver derivatives. In the Au_3Cu cores the $\text{Au}\cdots\text{Cu}$ distances are 2.9000(13)–2.9871(14) Å, which are slightly longer than

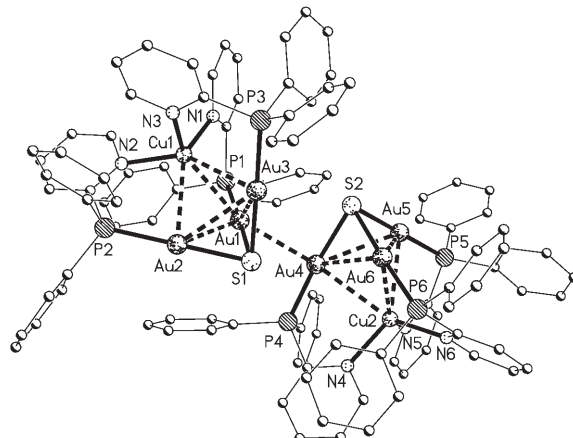


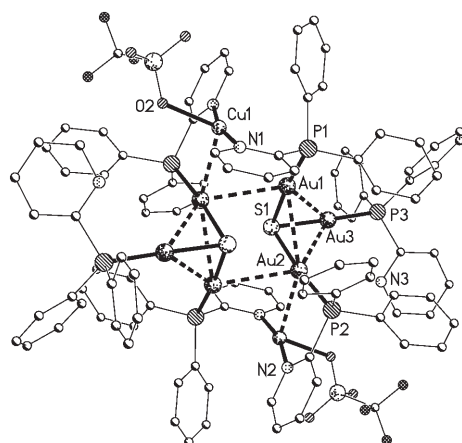
Figure 3. Structure of the cation of complex **11a**.

Table 2. Selected bond lengths [Å] and angles [°] for complex **11a**.

Au1–P1	2.258(3)	Au4–Au6	2.9989(5)
Au1–S1	2.358(3)	Au4–Au5	3.0034(5)
Au1–Au4	2.9496(6)	Au5–P5	2.244(3)
Au1–Au2	2.9801(6)	Au5–S2	2.323(3)
Au1–Cu1	2.9871(14)	Au5–Cu2	2.9166(13)
Au1–Au3	3.0000(6)	Au5–Au6	2.9949(6)
Au2–P2	2.244(3)	Au6–P6	2.252(3)
Au2–S1	2.326(2)	Au6–S2	2.331(3)
Au2–Cu1	2.9000(13)	Au6–Cu2	2.9151(14)
Au2–Au3	2.9854(5)	Cu1–N1	2.092(9)
Au3–P3	2.248(3)	Cu1–N2	2.115(8)
Au3–S1	2.323(3)	Cu1–N3	2.118(9)
Au3–Cu1	2.9056(13)	Cu2–N4	2.079(8)
Au4–P4	2.258(3)	Cu2–N5	2.110(8)
Au4–S2	2.354(3)	Cu2–N6	2.116(9)
Au4–Cu2	2.9737(13)		
P1–Au1–S1	175.69(10)	N4–Cu2–N5	104.8(3)
P2–Au2–S1	178.92(10)	N4–Cu2–N6	104.5(3)
P3–Au3–S1	178.49(10)	N5–Cu2–N6	101.8(3)
P4–Au4–S2	175.11(10)	Au3–S1–Au2	79.90(8)
P5–Au5–S2	178.67(10)	Au3–S1–Au1	79.71(8)
P6–Au6–S2	176.93(10)	Au2–S1–Au1	79.02(8)
N1–Cu1–N2	104.1(3)	Au5–S2–Au6	80.11(9)
N1–Cu1–N3	104.5(3)	Au5–S2–Au4	79.91(9)
N2–Cu1–N3	102.6(3)	Au6–S2–Au4	79.60(9)

those found in the complex $[\text{Cu}\{\text{Au}(\text{C}_6\text{F}_5)_2\}(\text{NCMe})(\mu_2\text{C}_4\text{H}_4\text{N}_2)]_n$, in which there is an unsupported $\text{Au}\cdots\text{Cu}$ interaction of 2.8216(6) Å,^[28] and longer than those in $[\text{AuCu}(\text{Spy})(\text{PPPh}_2\text{py})_2](\text{PF}_6)_2$, in which the shortest distances are 2.634(1) and 2.646(1) Å, indicating a bonding interaction.^[29] The $\text{Au}\cdots\text{S}$ distances are in the range 2.323(3)–2.358(3) Å, which are very similar to those found in the silver complex **8** (2.333(2)–2.337(1) Å). The intramolecular gold–gold interactions range from 2.9801(6) to 3.0000(6) Å, which are shorter than those found in the silver derivative (3.0661(3)–3.2096(3) Å). The $\text{Cu}\cdots\text{N}$ bond lengths are in the range 2.079(8)–2.118(9) Å.

The crystal structure of the cation of complex **11b** is shown in Figure 4 and a selection of bond lengths and angles is collected in Table 3. The structure is composed of

Figure 4. Structure of the cation of complex **11b**.Table 3. Selected bond lengths [Å] and angles [°] for complex **11b**.^[a]

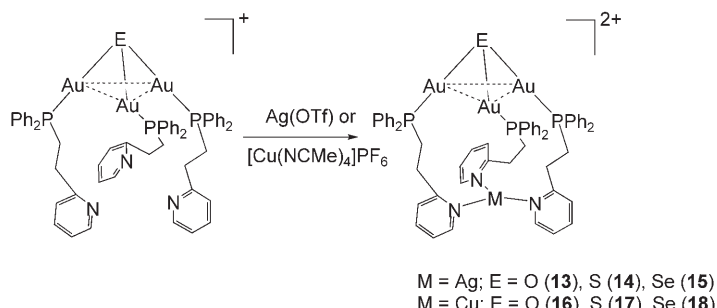
Au1–P1	2.2579(17)	Au2–Au1#1	3.1494(5)
Au1–S1	2.3309(16)	Au2–Au3	3.1566(5)
Au1–Au2	3.0633(4)	Au3–P3	2.2512(17)
Au1–Au2#1	3.1494(5)	Au3–S1	2.3030(17)
Au1–Au3	3.2568(5)	Cu1–N1	1.918(6)
Au2–P2	2.2633(19)	Cu1–N2#1	1.939(6)
Au2–S1	2.3414(18)	Cu1–O2#2	2.268(6)
Au2–Cu1#1	2.7954(9)		
P1–Au1–S1	173.83(6)	Au1#1–Au2–Au3	123.071(11)
Au2–Au1–Au2#1	89.713(10)	P3–Au3–S1	172.78(6)
Au2–Au1–Au3	59.835(11)	Au2–Au3–Au1	57.038(8)
Au2#1–Au1–Au3	121.613(10)	N1–Cu1–N2#1	164.6(2)
P2–Au2–S1	174.26(6)	N1–Cu1–O2#2	96.3(2)
Cu1#1–Au2–Au1	151.86(2)	N2#1–Cu1–O2#2	95.1(2)
Cu1#1–Au2–Au1#1	70.61(2)	Au3–S1–Au1	89.30(6)
Au1–Au2–Au1#1	90.287(10)	Au3–S1–Au2	85.63(6)
Cu1#1–Au2–Au3	109.66(2)	Au1–S1–Au2	81.94(5)
Au1–Au2–Au3	63.127(9)		

[a] Symmetry transformations used to generate equivalent atoms: #1: $-x+2, -y+2, -z+1$; #2: $-x+1, -y+2, -z+1$.

two SAu₃ units which bridge two copper atoms through the pyridine groups. The copper atoms are bonded to two nitrogen groups and the oxygen of the triflate anion with Cu–N distances of 1.918(6) and 1.939(6) Å, which are shorter than those in complex **11a** because the copper atoms are found in an irregular trigonal plane. There is only one Au···Cu bonding interaction of 2.7954(9), which is shorter than those found in the isomer **11a**. The other Cu···Au distance is 3.448 Å, too long to be considered as an interaction. However the gold–gold bonding distances are longer than those in complex **11a** and the range is 3.0633(4)–3.2568(5) Å. By comparing both structures we conclude that there are stronger Au···Au interactions and weaker Au···Cu interactions in isomer **11a** than in isomer **11b**.

We have also studied the reactivity of [E(AuPPh₂CH₂CH₂py)₃]BF₄ towards Ag(OTf) and [Cu(NCMe)₄]PF₆. Coordination to silver affords orange-red complexes of stoichiometry [E(AuPPh₂CH₂CH₂py)₃Ag](OTf)(BF₄) (E=O (**13**), S (**14**), Se (**15**)) and coordination to copper the pale yellow complexes [E(AuPPh₂CH₂CH₂py)₃Cu](BF₄)(PF₆) (E=O

(**16**), S (**17**), Se (**18**)) (Scheme 4). The ³¹P{¹H} NMR spectra of these complexes show one resonance, not very far from that in the starting material, suggesting similar structures



Scheme 4.

with the three pyridine groups bonded to the silver or copper atom. The chemical shift of the phosphorus atoms should not be significantly affected by coordination of the pyridine groups to the heterometal. The longer chain from the phosphorus to the nitrogen of the pyridine group in the heterofunctional ligand makes the formation of Au···M interactions difficult. This structure has been confirmed for one of the copper complexes in which Cu···Au interactions are absent. We assume that the silver complexes have a similar structure, although with the same stoichiometry different structures are possible. Furthermore, the color of the silver complexes indicates the presence of Ag···Au interactions and also their luminescence behavior does not follow the pattern shown by the copper complexes. Thus a similar structure to that found for the copper complex **11b** may be possible. Unfortunately, these complexes are not very stable in solution and decompose to form other side-products that do not contain the chalcogenide ion. No single crystals could be grown to unambiguously determine their structures.

The structure of complex **17** was confirmed by X-ray diffraction and the cation is shown in Figure 5. Selected bond lengths and angles are shown in Table 4. The copper atom is now coordinated only to the three nitrogen atoms in a regular trigonal planar coordination, with distances ranging from 1.986(9) to 2.021(8) Å and N–Cu–N angles of 123.7(3), 121.4(3), and 114.2(3)°. In the SAu₃ unit the gold–gold distances are 3.0287(6)–3.4127(6) Å, which are similar to those found in complex **11b**, and Au···Cu interactions are absent. The molecules arrange into dimers through intermolecular aurophilic interactions of 2.9518(8) Å (Figure 6).

Diffuse reflectance UV studies: The diffuse-reflectance UV (DRUV) spectra of solid samples of complexes **10–14** and **16–18** display similar profiles (see Table 5) with bands at around 275 nm and other bands and/or shoulders at lower energies (335–350 and 390–445 nm). Those at lower energies are similar in energy to those described by Yam et al. in $[\{Pt_2(\mu_3-E)_2(PPh_2py)_4\}_2Ag_3]^{3+}$ (E=S, Se)^[30] and in $[\{Pt_2(\mu_3-$

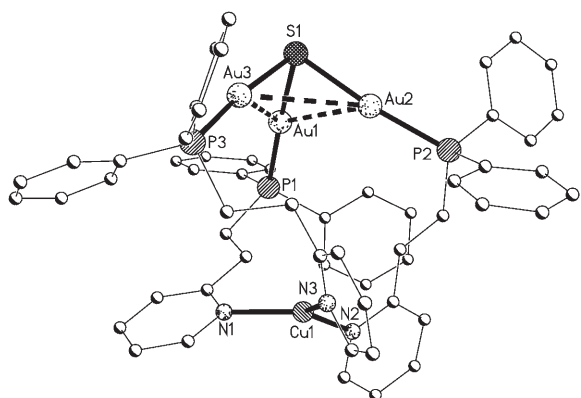


Figure 5. Structure of the cation of complex **17**.

Table 4. Selected bond lengths [\AA] and angles [$^\circ$] for complex **17**.^[a]

Au1-P1	2.260(3)	Au2-Au3	3.4127(6)
Au1-S1	2.335(3)	Au3-P3	2.266(3)
Au1-Au1#1	2.9518(8)	Au3-S1	2.318(3)
Au1-Au2	3.0287(6)	Au3-Au3#	13.2193(8)
Au1-Au3	3.2502(6)	Cu1-N3	1.986(9)
Au2-P2	2.263(3)	Cu1-N2	1.988(8)
Au2-S1	2.327(2)	Cu1-N1	2.021(8)
P1-Au1-S1	175.89(9)	Au3#1-Au3-Au2	129.749(14)
Au1#1-Au1-Au2	135.37(2)	Au1-Au3-Au2	54.007(12)
Au1#1-Au1-Au3	92.225(9)	N3-Cu1-N2	123.7(3)
Au2-Au1-Au3	65.737(13)	N3-Cu1-N1	121.4(3)
P2-Au2-S1	169.70(9)	N2-Cu1-N1	114.2(3)
Au1-Au2-Au3	60.256(13)	Au3-S1-Au2	94.55(9)
P3-Au3-S1	170.94(10)	Au3-S1-Au1	88.60(9)
Au3#1-Au3-Au1	87.519(9)	Au2-S1-Au1	81.02(8)

[a] Symmetry transformations used to generate equivalent atoms: #1: $-x+1, y, -z+\frac{1}{2}$.

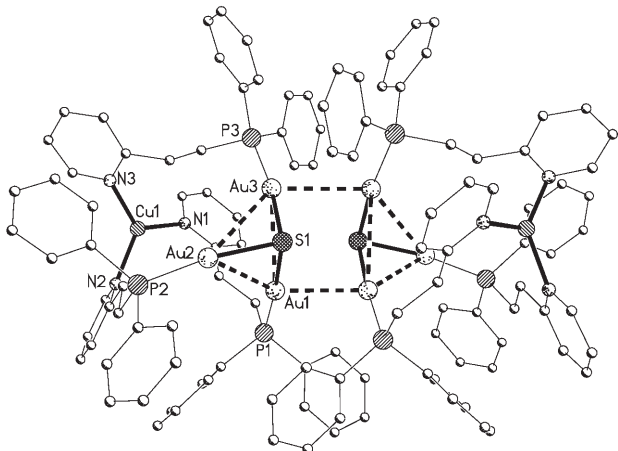


Figure 6. Formation of dimers in complex **17** through aurophilic interactions.

$\text{E}_2(\text{PPh}_2\text{py})_4\text{Ag}_2(\text{dppm})^{2+}$ which are in the range of 394–430 nm in MeCN solution at 298 K and may arise from ligand-to-metal charge transfer $[\text{E}^{2-}\rightarrow\text{Pt}]$ or $[\text{Pt}_2(\text{PPh}_2\text{py})_4(\mu_3-\text{E})\rightarrow\text{Pt}]$. Nevertheless LLCT $[\text{E}^{2-}\rightarrow\text{PPh}_2\text{py}]$ transitions cannot be ruled out. In these compounds the LMCT assign-

Table 5. Bands in the DRUV spectra of complexes $[\text{E}(\text{AuL})_3\text{Cu}]^{2+}$ in the solid state at room temperature.

Compound	Bands ^[a] [nm]
10	275, 345, 425 (sh)
11(BF₄)	280, 345, 440 (sh)
11(OTf)	265, 350, 455 (sh)
12	270, 350, 435 (sh)
13	275, 335, 390
14	275, 340, 385 (sh)
16	275, 330, 400 (sh)
17	280, 335
18	275, 335, 400 (sh)

[a] sh = shoulder

ment was made based on the shift to lower-energy absorption energies when changing the chalcogenide atom from sulfur to selenium. In our complexes no clear trends were observed, which may be related to the role of the M–N bonds in these molecules, as we point out below in the discussion on luminescence, taking into account the presence of the $[\text{EAu}_3\text{M}]$ core and the MN_x ($\text{M}=\text{Ag}, \text{Cu}$) unit in our complexes. In fact Goldberg et al. describe metal-to-ligand charge transfer (MLCT) bands in a similar region (345–415 nm) for CuN_4 chromophores^[31] in dichloromethane. A unique and simple origin does not explain the nature of these bands.

Luminescence studies: Two important structural features of $[\text{E}(\text{AuPR}_3)_3\text{M}]^{2+}$ must be taken into account to understand the luminescence properties of the complexes in the solid state (298 and 77 K). One is related to the presence of $\text{Au}\cdots\text{M}$ ($\text{M}=\text{Ag}, \text{Cu}$) interactions, depending on the monophosphine. When the monophosphine is PPh_2py the compounds display $\text{Au}\cdots\text{M}$ interactions, with two different structures found in the copper complexes. In the first one (**10a–12a**) the copper atom is bonded to the three nitrogen atoms and displays $\text{Cu}\cdots\text{Au}$ interactions with the three gold atoms. This is the arrangement shown by the silver derivatives (**7–9**) and is in a minor proportion for $[\text{E}(\text{AuPR}_3)_3\text{Cu}]^{2+}$ ($\text{E}=\text{O}, \text{Se}$ (**12**)). In the second structure (**10b–12b**) the copper atom is coordinated to two pyridine nitrogen atoms and displays only one $\text{Cu}\cdots\text{Au}$ interaction. This arrangement represents the major component of $[\text{E}(\text{AuPR}_3)_3\text{Cu}]^{2+}$ ($\text{E}=\text{O}$ (**10**), Se (**12**)). When $\text{E}=\text{S}$ (**11**) the counterion determines which form is the most important [i.e., BF_4^- and PF_6^- give a higher proportion of the first form (**11a**); OTf^- and PF_6^- mainly give the second form (**11b**)]. We measured the luminescence properties in the solid state and found that both isomers are present. However for complexes **10** and **12** we think that it is isomer **b** that mainly contributes to the luminescence (although quantum yields have not been measured). For compound **11** the ratio of the two isomers is different depending on the counteranion and for this reason both were measured. Clearly the origin of the luminescence seems to be similar since isomer **a** also dimerizes in the solid state and also this tendency agrees with that observed for silver. Compounds with $\text{PR}_3=\text{PPh}_2(\text{CH}_2)_2\text{py}$ show no

M···Au interactions and two different parts of the molecules should be considered, one is the “EAu₃” fragment and the other is the “MN₃” fragment (see Scheme 4).

The compounds [E(AuPPh₂py)₃Cu]²⁺ (E=O (**10**), S (**11**–OTf), Se (**12**)) show a significant red shift on going from oxygen to selenium (see Table 6; $\lambda_{\text{max}}(\text{emission}, 77 \text{ K}) = 584$

Table 6. Luminescent spectral data (λ_{max}) and lifetime measurements (τ) for compounds [E(AuPPh₂py)₃Cu]²⁺ at 298 and 77 K in the solid state.

E	λ [nm] (τ [μs])			
	289 K		77 K	
	excitation	emission	excitation	emission
O (10)			445	584
S [11(BF₄)] ^[a]	450	590 (24)	435	570
S [11(OTf)] ^[b]	370	590 (18.1)	435, 365	590, 620
	415	620		
Se (12)	360	650 (26.2)	439	652

[a] Majority isomer **a**. [b] Majority isomer **b**.

(E=O, **10**), 590, 620 (E=S, **11**(OTf)), 652 nm (E=Se, **12**)). Figure 7 shows the emission spectra of the complexes. The corresponding emission values observed for the analogous silver derivatives [E(AuPPh₂py)₃Ag]²⁺ show a larger red shift on going from oxygen to selenium ($\lambda_{\text{max}}(\text{emission}, 77 \text{ K}) = 482$ (E=O), 565 (E=S), 696 nm (E=Se)). These emissions have been attributed, predominantly, to a ligand-to-metal charge transfer (LMCT; E²⁻→Au₃Ag)^[24] triplet excited state, although a mixed nature, with the contribution of a metal-centered (MC, d-s or d-p) state is probable. Such emissions have also been observed in other polynuclear silver and copper complexes with chalcogenide bridging ligands.^[32] The fact that the ionization potentials of the chalcogen atoms increase from selenium to oxygen is in agreement with this explanation as it suggests a high contribution of the chalcogenide character to the donor orbital.

The emission spectrum of the triflate salt of compound **11** [S(AuPPh₂py)₃Cu](OTf)(PF₆) (mixture of isomers **a** and **b**) displays one band. The maximum of this band depends upon the excitation energy and moves from 620 (365) to 590 (435) nm. The one at 620 nm follows the pattern shown by the silver derivatives (an increase in the energy of the emission when E changes from selenium to oxygen). The higher energy emission maximum resembles the only one present in the tetrafluoroborate salt [S(AuPPh₂py)₃Cu](BF₄)(PF₆) (570 nm at 77 K, 590 nm at 298 K) (mainly isomer **a**). Thus, we propose LMCT (E²⁻→Au₃Cu) transitions as the main contribution to the emissions for compounds **10**, **11**(OTf), and **12**, in which the most important structure is the coordination isomer **b** (one Cu···Au interaction; two Cu–N bonds). This pattern follows that observed for the silver complexes [E(AuPPh₂py)₃Ag]²⁺. Compound **11**(BF₄), in which isomer **a** predominates, shows different maxima, which cannot be com-

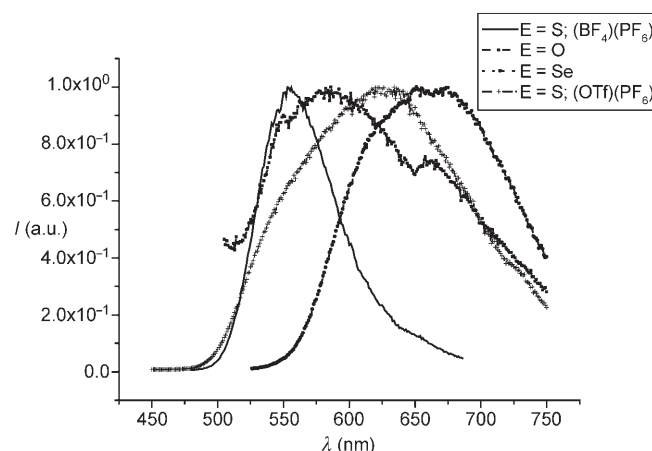


Figure 7. Emission spectra for compounds [E(AuPPh₂py)₃Cu]²⁺ at 77 K in the solid state.

pared with those of complexes **10** and **12** because this form is only a minor component in the oxygen and selenium derivatives.

Many luminescent copper systems have been studied including “CuN₄” chromophores;^[31] thus, contributions of the CuN₂ or CuN₃ (compound **11a**) systems to the luminescent properties of these complexes cannot be excluded.

In the compounds [E(AuPPh₂CH₂CH₂py)₃M]²⁺ (M=Cu, Ag) the larger monophosphine PPh₂CH₂CH₂py prevents a connection between the three gold atoms and the metal, silver, or copper.

Surprisingly, in the silver complexes [E(AuPPh₂CH₂CH₂py)₃Ag]²⁺ (E=O (**13**), S (**14**)) the emissions appear at lower energies (ca. 700 nm, Table 7, Figure 8). These values do not fit the trend that suggests a LMCT (E²⁻→Au₃Ag) origin for the transitions. Such an impressive change can be related to an important change in the structure of the complexes. In order to understand these values we have considered the “AgN₃” system in the molecule and tried to study its contribution to the emissions. With this aim we synthesized [Ag(NC₅H₃Me₂)₃]⁺, (NC₅H₃Me₂=2,6-lutidine) in which no silver···silver interactions are present and the compound is not luminescent. On the other hand, systems with 2-aminomethylpyridine^[33] show emissions in the 390–480 nm region; the authors of this work proposed a ligand-based absorption which decays by means of ligand-to-metal charge transfer. Thus, it is unlikely that this is the origin of the emissions in

Table 7. Luminescent spectral data (λ_{max}) and lifetime measurements (τ) for compounds [E(AuPPh₂CH₂CH₂py)₃M]²⁺ [M=Ag (**13,14**), Cu (**16–18**)] at 298 and 77 K in the solid state.

E	M=Ag				M=Cu			
	298 K		77 K		298 K		77 K	
	excitation	emission	excitation	emission	excitation	emission	excitation	emission
O			410	701	359	520 (11.8)	349	525
S	473	725 (12.6)	550	725	365	540 (24.3)	367	535
Se					360	560 (11.7)	363	570

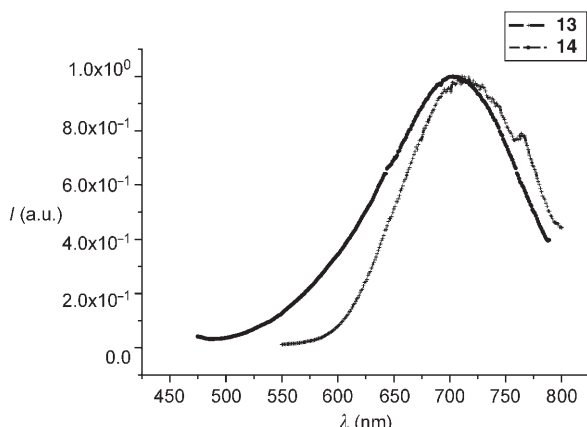


Figure 8. Emission spectra for compounds $[E(AuPPh_2CH_2CH_2py)_3Ag]^{2+}$ at 77 K in the solid state.

the complexes of this study, rather Au···Ag interactions may be the origin.

Our preliminary studies on “[Au_m{PPh₂(CH₂)₂py}]_n” systems show emissions at higher energies ($\lambda_{\text{max}}=600$ nm). The $[[Pt_2(\mu_3-E)_2(PPh_2py)_4]Ag_3]^{3+}$ (E=S, Se) and $[[Pt_2(PPh_2py)_4-(\mu_3-E)_2Ag_2(dppm)]^{2+}$ systems^[30] show luminescence with $\lambda_{\text{max}}>600$ nm. In these systems the emissions have been assigned to $E^{2-}\rightarrow Ag$ transitions, with possible contributions from $E^{2-}\rightarrow Pt$, although another possibility is $[Pt_2(dppm)_4(\mu_3-E)_2]\rightarrow Ag$.

When M=Cu the emissions exhibit the pattern discussed above (see Table 7, Figure 9) ($\lambda_{\text{max}}(\text{emission}, 77 \text{ K})=525$ (E=O, **16**), 535 (E=S, **17**), 570 nm (E=Se, **18**)). Nevertheless, there is a smaller shift to the red in the emissions. In the previous complexes (**10–12**) the coordination of M to “E(AuPPh₂py)₃” seems to be responsible for the intensity of the emissions. In these copper complexes the absence of M···Au interactions and the smaller shift to the red when changing from oxygen to selenium suggest an important contribution of the CuN₃ core to the emissions.

Conclusion

Heteropolynuclear chalcogenide gold complexes have been prepared by reactions of the trigold complexes $[E-(AuPPh_2py)_3]^+$ or $[E(AuPPh_2CH_2CH_2py)_3]^+$ (E=O, S, Se) with silver or copper compounds. Different results were found, depending on the metal and the heterofunctional phosphine ligand. With PPh₂py, silver tetrahedral Au₃M clusters were obtained, whereas with copper two coordination isomers with different metallophilic interactions were obtained, one of them analogous to that of silver. With PPh₂CH₂CH₂py, which has a longer chain, no metallophilic interactions were found and the silver or copper atom coordinates to three nitrogen atoms. All these $[E(AuL)_3M]^{2+}$ complexes display interesting luminescence properties that have been studied by variation of three factors: the chalcogenide (E), the heterofunctional ligand (L), and the metal (M). The chalcogenide influences the emission energies which vary from blue for oxygen to green for sulfur to orange for selenium. The metallophilic interactions vary with the heterofunctional ligand and the metal. The emissions have been attributed, predominantly, to a ligand-to-metal charge transfer (LMCT; $E^{2-}\rightarrow Au_3M$) triplet excited state, although a mixed nature, with a contribution from a metal-centered (MC, d-s or d-p) state is probable for $[E-(AuPPh_2py)_3M]^{2+}$ systems. For the $[E(AuPPh_2CH_2CH_2py)_3Cu]^{2+}$ complexes the CuN₃ unit seems to make a very important contribution to the emissions, while in $[E(AuPPh_2CH_2CH_2py)_3Ag]^{2+}$ the nature of the emissions seems to be more complex.

Experimental Section

Instrumentation: Infrared spectra were recorded in the range 4000–200 cm⁻¹ with a Perkin–Elmer 883 spectrophotometer using Nujol mulls between polyethylene sheets. Conductivities of solutions (ca. 5×10^{-4} mol dm⁻³) were measured with a Philips 9509 conductimeter. C, H, N, and S analyses were carried out with a Perkin–Elmer 2400 microanalyzer. Mass spectra were recorded with a VG Autospec spectrometer using the liquid secondary-ion mass spectra (LSIMS) technique with nitrobenzyl alcohol as the matrix. NMR spectra were recorded with Varian Unity 300 and Bruker ARX 300 spectrometers. Chemical shifts are cited relative to SiMe₄ (¹H, external), CFCl₃ (¹⁹F, external), and 85% H₃PO₄ (³¹P, external). DRUV spectra were recorded with a Unicam UV-4 spectrophotometer equipped with a Spectralon RSA-UC-40 Labsphere integrating sphere. The solid samples were mixed with dried KBr to form an homogeneous powder. The mixtures were placed in a home-made cell equipped with a quartz window. The intensities were recorded in Kubelka–Munk units: $\log[R/(1-R)^2]$, where R=reflectance. Steady-state photoluminescence spectra were recorded with a Jobin–Yvon Horiba Fluorolog FL-3–11 spectrometer using band pathways of 3 nm for both excitation and emission. Phosphorescence lifetimes were recorded with a Fluoromax phosphorimeter accessory containing a UV xenon flash tube at a flash rate between 0.05 and 25 Hz. The lifetime data were fitted using the Jobin–Yvon software package^[34] and the Origin 5.0 program.^[35]

Starting materials: The starting materials PPh₂CH₂CH₂py,^[36] [AuCl(PPh₂py)],^[37] and [Cu(NCMe)₄]PF₆,^[38] were prepared according to published procedures. All other reagents were commercially available. [AuCl(PPh₂CH₂CH₂py)] was prepared by reaction of [AuCl(tht)]^[39] (THT=tetrahydrothiophene) with PPh₂CH₂CH₂py in dichloromethane.

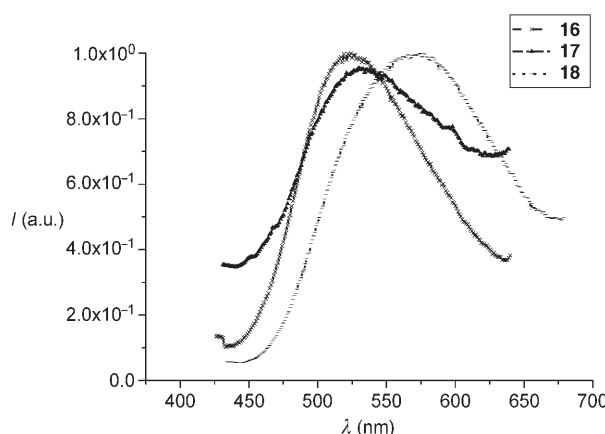


Figure 9. Emission spectra for compounds $[E(AuPPh_2CH_2CH_2Py)_3Cu]^{2+}$ at 77 K in the solid state.

[Au(OTf)(PPh₂py)] was prepared from [AuCl(PPh₂py)] by reaction with Ag(OTf) in dichloromethane and used in situ. [S(AuPPh₂py)₂] was prepared by the method described for the synthesis of [S(AuPPh₃)₂].^[40]

Synthesis of [O(AuPPh₂py)₃]BF₄ (1) and [O(AuPPh₂CH₂CH₂py)₃]BF₄ (2): Silver oxide was prepared by adding a solution of sodium hydroxide (0.45 g, 11.2 mmol) in water (10 mL) to a solution of silver nitrate (1.88 g, 11.0 mmol) in water (10 mL). The brown precipitate was removed by filtration through a glass frit, washed with water (2 × 5 mL), ethanol (2 × 5 mL), and acetone (2 × 5 mL), and air-dried. The freshly prepared solid silver oxide was added to a 250 mL round-bottomed flask containing a solution of [AuCl(PPh₂py)] (1.487 g, 3 mmol) or [AuCl(PPh₂CH₂CH₂py)] (1.570 g, 3 mmol) in acetone (100 mL), together with a magnetic stirring bar. This was followed by the addition of NaBF₄ (1.866 g, 17.1 mmol). The mixture was stirred for 3 h, the acetone removed, and the solid residue extracted with dichloromethane (3 × 15 mL). The combined extracts were evaporated to leave around 5 mL and addition of diethyl ether gave a white solid of complex **1** or **2**.

Complex **1** (87 %, 1.29 g): ³¹P{¹H} NMR (CDCl₃): δ = 23.4 ppm; ¹H NMR (CDCl₃): δ = 8.69 (d, ³J_{H,H} = 4.4 Hz, 3H; py), 7.73–7.61 (m, 18H; Ph), 7.51 (m, 6H; py), 7.42 (m, 3H; py), 7.37–7.34 ppm (m, 12H; Ph); elemental analysis calcd (%) for C₅₁H₄₂Au₃BF₄N₃OP₃: C 40.46, H 1.57, N 1.57; found: C 40.23, H 1.45, N 1.62.

Complex **2** (70%, 1.097 g): ³¹P{¹H} NMR (CDCl₃): δ = 21.13 ppm; ¹H NMR (CDCl₃): δ = 8.40 (m, 3H; py), 7.73–7.00 (m, 30 + 9H; Ph + py), 3.06 (m, 6H; CH₂), 2.96 ppm (m, 6H; CH₂); MS (LSIMS+): m/z (%): 1480 (5) [O(AuPPh₂CH₂CH₂py)₃]⁺; elemental analysis calcd (%) for C₅₇H₅₄Au₃BF₄N₃OP₃: C 43.65; H 3.44, N 2.68; found: C 43.60, H 3.03, N 2.70.

Synthesis of [S(AuPPh₂py)₃]X [X = OTf (**3a**), BF₄ (**3b**)], [Se(AuPPh₂py)₃]BF₄ (**4**), and [E(AuPPh₂CH₂CH₂py)₃]BF₄ [E = S (**5**), Se (**6**)]:

Method A: To a solution of [S(AuPPh₂py)₂] (0.108 g, 0.1 mmol) in CH₂Cl₂ (20 mL) was added [Au(OTf)(PPh₂py)] (0.073 g, 0.12 mmol) in excess, and the solution stirred at room temperature for 30 min. Evaporation of the solvent to around 5 mL and addition of diethyl ether gave **3a** as a white solid.

Method B: Complex **1** (0.148 g, 0.1 mmol) or **2** (0.156, 0.1 mmol) and SC(NH₂)₂ (0.007 g, 0.1 mmol) or SeC(NH₂)₂ (0.012 g, 0.1 mmol) were dissolved in acetone (20 mL) and the solution stirred for 3 h. After this time, concentration of the solution to 5 mL and addition of diethyl ether gave **3b–6** as white solids.

Complex **3a** (83 %, 0.130 g): ³¹P{¹H} NMR (CDCl₃): δ = 32.37 ppm; ¹H NMR (CDCl₃): δ = 8.47 (m, 3H; py), 7.56–7.19 ppm (m, 30 + 9, Ph + py); MS (LSIMS+): m/z (%): 1412 (100) [S(AuPPh₂py)₃]⁺; elemental analysis calcd (%) for C₅₂H₄₂Au₃F₃N₃O₃P₃S₂: C 39.99, H 2.71, N 2.69, S 4.11; found: C 39.74, H 2.69, N 2.70, S 3.81.

Complex **3b** (86 %, 0.129 g): elemental analysis calcd (%) for C₅₁H₄₂Au₃BF₄N₃P₃S: C 40.84, H 2.82, N 2.80, S 2.13; found: C 40.65, H 2.67, N 2.75, S 2.04.

Complex **4** (84 %, 0.129 g): ³¹P{¹H} NMR (CDCl₃): δ = 33.60 ppm; ¹H NMR (CDCl₃): δ = 8.48 (m, 3H; py), 7.59–7.19 ppm (m, 30 + 9, Ph + py); MS (LSIMS+): m/z (%): 1460 (85) [Se(AuPPh₂py)₃]⁺. Elemental analysis calcd (%) for C₅₁H₄₂Au₃BF₄N₃P₃Se: C 39.57, H 2.71, N 2.71; found: C 39.50, H 2.70, N 2.73.

Complex **5** (81 %, 0.129 g): ³¹P{¹H} NMR (CDCl₃): δ = 29.76 ppm; ¹H NMR (CDCl₃): δ = 8.39 (br d, ³J_{H,H} = 4 Hz, 3H; py), 7.64–7.59 (m, 12H; Ph), 7.50 (m, 3H; py), 7.39 (m, 6H; Ph), 7.24 (m, 12H; Ph), 7.09 (m, 3H; py), 6.95 (br d, ³J_{H,H} = 7.60 Hz, 3H; py), 2.97 ppm (m, 12H; CH₂); elemental analysis calcd (%) for C₅₇H₅₄Au₃BF₄N₃P₃S: C 43.65, H 3.44, N 2.68; S 2.68; found: C 43.68, H 3.55, N 2.65, S 2.41.

Complex **6** (81 %, 0.129 g): ³¹P{¹H} NMR (CDCl₃): δ = 31.44 ppm; ¹H NMR (CDCl₃): δ = 8.39 (br d, ³J_{H,H} = 4.4 Hz, 3H; py), 7.58 (m, 12H; Ph), 7.47 (m, 3H; py), 7.36 (m, 6H; Ph), 7.19 (m, 12H; Ph), 7.09 (m, 3H; py), 6.91 (d, ³J_{H,H} = 7.60 Hz, 3H; py), 2.93 ppm (m, 12H; CH₂); MS (LSIMS+): m/z (%): 1544 (5) [Se(AuPPh₂(CH₂)₂py)₃]⁺; elemental analysis calcd (%) for C₅₇H₅₄Au₃BF₄N₃P₃Se: C 44.33, H 3.49, N 2.72; found: C 44.09, H 3.51, N 2.71.

Synthesis of [O(AuPPh₂py)₃Ag](BF₄)₂ (7**):** To a solution of **1** (0.148 g, 0.1 mmol) in dichloromethane (20 mL) was added AgBF₄ (0.019 g, 0.1 mmol) and the solution was stirred for 30 min. Concentration of the solution around 5 mL and the addition of diethyl ether gave a pale yellow solid (86 %, 0.144 g). ³¹P{¹H} NMR (CD₂Cl₂): δ = 28.03 ppm; ¹H NMR (CDCl₃): δ = 7.77 (m, 6H; py), 7.54–7.40 (m, 30H; Ph), 7.18 (m, 3H; py), 7.06 ppm (m, 3H; py); elemental analysis calcd (%) for C₅₁H₄₂AgAu₃B₂F₈N₃OP₃: C 36.47, H 2.50, N 2.50; found: C 36.23, H 2.22, N 2.27.

Synthesis of [S(AuPPh₂py)₃Ag](OTf)₂ (8**):** A solution of **3** (0.156 g, 0.1 mmol) and AgOTf (0.026 g, 0.1 mmol) in dichloromethane (20 mL) was stirred at room temperature for 30 min and the solution turned orange. Concentration of the solution to ca. 5 mL and addition of diethyl ether gave a yellow solid (89 %, 0.161 g). ³¹P{¹H} NMR (CD₂Cl₂): δ = 37.39 ppm; ¹H NMR (CDCl₃): δ = 7.87 (m, 3H; py), 7.76 (m, 3H; py), 7.50–7.39 (m, 30H; Ph), 7.30 (m, 3H; py), 7.11 ppm (m, 3H; py); MS (LSIMS+): m/z (%): 1670 (10) [S(AuPPh₂py)₃AgOTf]⁺; elemental analysis calcd (%) for C₅₃H₄₂AgAu₃F₆N₃O₆P₃S₂: C 34.99, H 2.33, N 2.31, S 5.28; found: C 34.91, H 2.23, N 2.12, S 4.98.

Synthesis of [Se(AuPPh₂py)₃Ag](BF₄)(OTf) (9**):** AgOTf (0.026 g, 0.1 mmol) was added to a solution of **4** (0.154 g, 0.1 mmol) in dichloromethane (20 mL), the solution turned yellow, and the solution was stirred at room temperature for 30 min. Concentration of the solution to around 5 mL and addition of diethyl ether gave a yellow solid (76 %, 0.1365 g). ³¹P{¹H} NMR (CD₂Cl₂): δ = 40.51 ppm; ¹H NMR (CDCl₃): δ = 7.79 (m, 3H; py), 7.58–7.47 (m, 30 + 3H; Ph + py), 7.23 (m, 3H; py), 7.04 ppm (m, 3H; py); elemental analysis calcd (%) for C₅₂H₄₂AgAu₃BF₄N₃O₃P₃SSe: C 34.63, H 2.34, N 2.33; Se 1.77; found: C 34.71, H 2.18; N 2.47; Se 1.49.

Synthesis of [O(AuPPh₂py)₃Cu](BF₄)(PF₆) (10**):** [Cu(NCMe)₄]PF₆ (0.037 g, 0.1 mmol) was added to a solution of **1** (0.148 g, 0.1 mmol) in dry CH₂Cl₂ (20 mL) and the mixture was stirred for 30 min. Concentration of the solution to around 5 mL and addition of diethyl ether gave **10** (92 %, 0.156 g) as a yellow solid. ³¹P{¹H} NMR [(CD₃)₂CO]: δ = 31.4 (s, 2P), 26.8 ppm (s, 4P); ¹H NMR (CDCl₃): δ = 9.35 (br m, 6H; py), 8.65 (br m, 6H; py), 8.35 (br m, 6H; py), 7.99 (br m, 6H; py), 7.49–7.61 ppm (m, 30H; Ph); elemental analysis calcd (%) for C₅₀H₄₂CuAu₃BF₁₀N₃OP₄: C 35.75, H 2.52, N 2.50; found: C 35.65, H 2.47, N 2.34.

Synthesis of [S(AuPPh₂py)₃Cu](BF₄)(PF₆) (11**):** [Cu(NCMe)₄]PF₆ (0.037 g, 0.1 mmol) was added to a solution of **3b** (0.149 g, 0.1 mmol) in dry dichloromethane (20 mL) and the solution turned yellow. The mixture was stirred for 30 min, after this time, concentration of the solution to around 5 mL and addition of diethyl ether gave a yellow solid (75 %, 0.128 g). ³¹P{¹H} NMR [(CD₃)₂CO]: T = 298 K, δ = 35.19 ppm; 273 K, δ = 36.9, 34.8 ppm; 253 K, δ = 35.8 and 32.4 (isomer **11b**), 33.7, 32.7, 30.9 ppm (isomer **11a**); 233 and 213 K, δ = 35.8 and 32.4 (isomer **11b**), 33.7, 32.7, 30.9 ppm (isomer **11a**); 193 K, δ = 35.3 (br, isomer **11b**), 33.8, 32.5, 29.9 ppm (isomer **11a**); ¹H NMR (CDCl₃): δ = 7.4–8.3 ppm (br m, py + Ph); elemental analysis calcd (%) for C₅₁H₄₂Au₃BCuF₁₀N₃P₄S: C 35.86, H 2.47, N 2.46, S 1.87; found: C 35.60, H 2.35, N 2.28, S 1.96.

Synthesis of [S(AuPPh₂py)₃Cu](OTf)(PF₆) (11**):** [Cu(NCMe)₄]PF₆ (0.037 g, 0.1 mmol) was added to a solution of **3a** (0.156 g, 0.1 mmol) in dry dichloromethane (20 mL) and the solution turned yellow. The mixture was stirred for 30 min, after this time, concentration of the solution to around 5 mL and addition of diethyl ether gave a yellow solid (71 %, 0.137 g). ³¹P{¹H} NMR [(CD₃)₂CO]: T = 298 K, δ = 35.2 ppm (br); 273 K, δ = 36.3, 33.4 ppm; 253 K, δ = 36.0 and 32.9 (isomer **11b**), 33.7, 32.9, 31.3 ppm (isomer **11a**); 233 and 213 K, δ = 35.8 and 32.7 (isomer **11b**), 33.7, 32.7, 30.9 ppm (isomer **11a**); 193 K, δ = 35.3 (br, isomer **11b**), 33.8, 32.5, 29.9 ppm (isomer **11a**); ¹H NMR (CDCl₃): δ = 7.4–8.3 ppm (br m, py + Ph); MS (LSIMS+): m/z (%): 1624 (5) [S(AuPPh₂py)₃Cu](OTf)⁺; elemental analysis calcd (%) for C₅₃H₄₂Au₃CuF₉N₃O₃P₄S₂: C 35.27, H 2.39, N 2.37, S 3.62; found: C 35.20, H 2.15, N 2.28, S 3.30.

Synthesis of [Se(AuPPh₂py)₃Cu](BF₄)(PF₆) (12**):** [Cu(NCMe)₄]PF₆ (0.037 g, 0.1 mmol) was added to a solution of **4** (0.154 g, 0.1 mmol) in dry dichloromethane (20 mL) and the solution turned yellow. The mixture was stirred for 30 min and after concentration of the solution to about 5 mL addition of diethyl ether resulted in the precipitation of a yellow solid (85 %, 0.150 g). ³¹P{¹H} NMR [(CD₃)₂CO]: δ = 38.2 (br, 4P),

34.9 ppm (br, 2P); ^1H NMR (CDCl_3): δ =8.2–7.4 ppm (m, 12+30H; py+Ph); elemental analysis calcd (%) for $\text{C}_{51}\text{H}_{42}\text{Au}_3\text{BCuF}_{10}\text{N}_3\text{P}_4\text{Se}$: C 34.90, H 2.41, N 2.39; found: C 34.62, H 2.39, N 2.40.

Synthesis of [E(AuPPh₂CH₂CH₂py)₃Ag](BF₄)(OTf) (E=O (13), S (14), Se (15)): AgOTf (0.025 g, 0.1 mmol) was added to a solution of **2** (0.156 g, 0.1 mmol), **5** (0.158 g, 0.1 mmol), or **6** (0.163 g, 0.1 mmol) in dichloromethane (20 mL) and the solution turned yellow (**13**, **14**) or orange (**15**). The mixture was stirred at room temperature for 30 min, and concentration of the solution to around 5 mL followed by addition of hexane gave a yellow (**13**), orange (**14**), or red solid (**15**).

Complex **13** (87 %, 0.158 g): $^{31}\text{P}\{^1\text{H}\}$ NMR [(CD_3)₂CO]: δ =29.37 ppm (s, 3P); ^1H NMR (CDCl_3): δ =8.43 (m, 3H; py), 7.85 (m, 12H; Ph), 7.68–7.36 (m, 18+3H; Ph+py), 7.16 (m, 6H; py) 3.26 (m, 6H; CH₂), 3.14 ppm (m, 6H; CH₂); elemental analysis calcd (%) for $\text{C}_{58}\text{H}_{54}\text{AgAu}_3\text{BF}_7\text{N}_3\text{O}_4\text{P}_3\text{S}$: C 38.18, H 2.98, N 2.30; S 1.75; found: C 38.25; H 2.59; N 2.33; S 1.47.

Complex **14** (53 %, 0.098 g): $^{31}\text{P}\{^1\text{H}\}$ NMR [(CD_3)₂CO]: δ =30.4 ppm (s, 3P); ^1H NMR (CDCl_3): δ =8.48 (m, 3H; py), 7.88 (m, 3H; py), 7.76–7.29 (m, 30+6, Ph+py), 3.36 (m, 6H; CH₂), 3.17 ppm (m, 6H; CH₂); elemental analysis calcd (%) for $\text{C}_{58}\text{H}_{54}\text{AgAu}_3\text{BF}_7\text{N}_3\text{O}_3\text{P}_3\text{S}_2$: C 37.82, H 2.93, N 2.28; S 3.47; found: C 37.84; H 2.72; N 2.16; S 3.51.

Complex **15** (30 %, 0.056 g): $^{31}\text{P}\{^1\text{H}\}$ NMR [(CD_3)₂CO]: δ =32.38 ppm; ^1H NMR [(CD_3)₂CO]: δ =8.42 (m, 3H; py), 7.91–7.13 (m, 30+9H; Ph+py), 3.30 (m, 6H; CH₂), 3.19 ppm (m, 6H; CH₂); elemental analysis calcd (%) for $\text{C}_{58}\text{H}_{54}\text{AgAu}_3\text{BF}_7\text{N}_3\text{O}_3\text{P}_3\text{SSe}$: C 36.90, H 2.88, N 2.22, Se 1.70; found: C 37.05; H 2.71; N 2.13, Se 1.82.

Synthesis of [E(AuPPh₂CH₂CH₂py)₃Cu](BF₄)(PF₆) (E=O (16), S (17), Se (18)): [Cu(NCMe)₄]PF₆ (0.037 g, 0.1 mmol) was added to a solution of **2** (0.156 g, 0.1 mmol), **5** (0.158 g, 0.1 mmol), or **6** (0.163 g, 0.1 mmol) in dry dichloromethane (20 mL). The solution was stirred for 30 min, during this time, the mixture turned pale yellow (**16**, **17**) or orange (**18**). Concentration of the solution to around 5 mL and addition of hexane gave a yellow (**16**, **17**) or orange precipitate (**18**).

tration of the solution to around 5 mL and addition of hexane gave a yellow (**16**, **17**) or orange precipitate (**18**).

Complex **16** (55 %, 0.097 g): $^{31}\text{P}\{^1\text{H}\}$ NMR [(CD_3)₂CO]: δ =30.0 ppm; ^1H NMR (CDCl_3): δ =8.86 (d, $^3J_{\text{H,H}}$ =4.6 Hz, 3H; py), 8.23 (“t”, $^3J_{\text{H,H}}$ =7.5 Hz, 3H; py), 7.75 (“t”, $^3J_{\text{H,H}}$ =6.4 Hz, 3H; py), 8.01–7.57 (m, 3+30H; py+Ph), 4.05 (m, 6H; CH₂), 3.66 ppm (m, 6H; CH₂); elemental analysis calcd (%) for $\text{C}_{57}\text{H}_{54}\text{Au}_3\text{BCuF}_{10}\text{N}_3\text{P}_4\text{O}$: C 38.54, H 3.06, N 2.36; found: C 38.72, H 3.34, N 2.0.

Complex **17** (70 %, 0.125 g): $^{31}\text{P}\{^1\text{H}\}$ NMR (CD_2Cl_2): δ =29.98 ppm; ^1H NMR (CDCl_3): δ =8.18 (m, 3H; py), 7.76 (m, 3H; py), 7.62–7.33 (m, 30H; Ph), 7.24 (m, 3H; py), 7.10 (m, 3H; py), 2.95 (m, 6H; CH₂), 2.81 ppm (m, 6H; CH₂); elemental analysis calcd (%) for $\text{C}_{57}\text{H}_{54}\text{Au}_3\text{BCuF}_{10}\text{N}_3\text{P}_4\text{S}$: C 38.19, H 3.05, N 2.35; S 1.79; found: C 38.38, H 3.00, N 1.98; S 1.76.

Complex **18** (40 %, 0.073 g): $^{31}\text{P}\{^1\text{H}\}$ NMR [(CD_3)₂CO]: δ =32.73 ppm; ^1H NMR (CDCl_3): δ =8.42 (m, 3H; py), 7.91–7.47 (m, 30+6H; Ph+py), 7.35 (m, 3H; py), 3.28 (m, 6H; CH₂), 3.17 ppm (m, 6H; CH₂); elemental analysis calcd (%) for $\text{C}_{57}\text{H}_{54}\text{Au}_3\text{BCuF}_{10}\text{N}_3\text{P}_4\text{Se}$: C 37.20, H 2.93, N 2.28; found: C 37.45 H, 3.08, N 2.41.

Crystal structure determinations: Data were recorded on a Bruker Smart Apex CCD diffractometer. The crystals were mounted in inert oil on glass fibres and transferred to the cold gas stream of the diffractometer. Data were collected using monochromated Mo_{Kα} radiation (λ =0.71073 Å) with ω and φ scans. An absorption correction based on multiple scans was applied using the SADABS program.^[41] The structures were solved by direct methods and refined on F^2 using the SHELXL-97 program.^[42] All non-hydrogen atoms were refined anisotropically. Hydrogen atoms were included using a riding model. Further crystal data are given in Table 8 and Table 9.

CCDC-604161 -604166 contain the supplementary crystallographic data for this paper. These data can be obtained free of charge from The Cam-

Table 8. X-ray data for complexes **1**, **2**, and **4**.

Compound	1	2	4
formula	$\text{C}_{51}\text{H}_{42}\text{Au}_3\text{F}_6\text{N}_3\text{OP}_4$	$\text{C}_{57}\text{H}_{52}\text{Au}_3\text{BF}_4\text{N}_3\text{OP} \cdot \text{CH}_2\text{Cl}_2$	$\text{C}_{102}\text{H}_{84}\text{Au}_6\text{B}_2\text{F}_8\text{N}_6\text{P}_6\text{Se}_2$
M_r	1541.66	1650.56	3092.91
habit	colorless prism	colorless prism	pale yellow needle
crystal size [mm]	0.30×0.25×0.19	0.40×0.40×0.32	0.90×0.20×0.16
crystal system	monoclinic	monoclinic	monoclinic
space group	$P2_1/c$	$P2_1/n$	$P2_1/n$
cell constants:			
a [Å]	12.4876(17)	13.8929(9)	17.843(5)
b [Å]	24.364(3)	18.9062(13)	25.731(6)
c [Å]	15.856(2)	21.5371(15)	21.318(5)
α [°]	90	90	90
β [°]	97.253	101.164(1)	96.409(4)
γ [°]	90	90	90
V [Å ³]	4785.4(11)	5549.9(7)	9726(4)
Z	4	4	4
ρ_{calcd} [Mg m ⁻³]	2.140	1.975	2.112
μ [mm ⁻¹]	9.375	8.151	9.93
$F(000)$	2912	3152	5808
T [°C]	-173	-173	-173
$2\theta_{\text{max}}$ [°]	57	57	57
no. of refl.:			
measured	30259	36657	62702
independent	10929	13074	22256
transmissions	0.165–0.269	0.14–0.18	0.04–0.299
R_{int}	0.056	0.028	0.072
parameters	613	676	1189
restraints	93	0	189
$wR(F^2)$ (all refl.)	0.136	0.067	0.134
R [$I > 2\sigma(I)$]	0.058	0.028	0.051
S	1.043	1.042	1.022
$\Delta\rho_{\text{max}}$ [e Å ⁻³]	3.08	2.32	4.10

Table 9. X-ray data for complexes **11a**, **11b**, and **17**.

Compound	11a	11b	17
formula	C ₁₀₂ H ₈₂ Au ₆ Cu ₂ F ₂₁ N ₆ O ₃ P ₉ S ₃ ·7ClCH ₂ CH ₂ Cl	C ₅₂ H ₄₂ Au ₃ CuF ₉ N ₃ O ₃ P ₄ S ₂ ·2CH ₂ Cl ₂	C ₅₇ H ₅₄ Au ₃ BCuF ₁₀ N ₃ P ₄ S
M _r	4215.19	1869.28	1792.22
habit	yellow prism	yellow prism	colorless needle
crystal size [mm]	0.20×0.16×0.12	0.20×0.16×0.14	0.28×0.08×0.04
crystal system	triclinic	triclinic	monoclinic
space group	P $\bar{1}$	P $\bar{1}$	C2/c
cell constants:			
<i>a</i> [Å]	14.1613(6)	14.0228(15)	24.167(2)
<i>b</i> [Å]	16.3672(7)	15.7577(17)	16.0731(14)
<i>c</i> [Å]	30.2682(14)	15.9007(17)	29.747(3)
α [°]	87.4980(10)	72.649(2)	90
β [°]	85.8210(10)	70.771(2)	95.705(2)
γ [°]	84.5240(10)	65.966(2)	90
<i>V</i> [Å ³]	6960.2(5)	2974.5(6)	11497.4(17)
<i>Z</i>	2	2	8
ρ_{calcd} [Mg m ⁻³]	2.011	2.087	2.071
μ [mm ⁻¹]	7.093	8.069	8.219
<i>F</i> (000)	4028	1776	6832
<i>T</i> [°C]	-173	-173	-173
2 θ _{max} [°]	50	57	57
no. of refl.:			
measured	71136	34207	37846
independent	24452	13596	13569
transmissions	0.336–0.483	0.295–0.397	0.766–1.0
<i>R</i> _{int}	0.042	0.036	0.088
parameters	1621	776	721
restraints	227	42	567
wR(<i>F</i> ²) (all refl.)	0.144	0.103	0.131
<i>R</i> [<i>I</i> >2σ(<i>I</i>)]	0.050	0.041	0.059
<i>S</i>	1.025	1.042	0.995
Δρ _{max} [e Å ⁻³]	2.61	3.56	2.78

bridge Crystallographic Data Centre via www.ccdc.cam.ac.uk/data_request/cif.

Acknowledgements

We thank the Ministerio de Educación y Ciencia (BQU2004-05495-C02-01) for financial support. We thank R. Eisenberg, H. J. Gysling and Q. M. Wang for fruitful discussions and E. Vispe for his explanations relating to the DRUV equipment.

- [1] C. H. Chen, J. Shi, *Coord. Chem. Rev.* **1998**, *171*, 161.
- [2] S. Sibley, M. E. Thompson, P. E. Burrows, S. R. Forrest in *Optoelectronic Properties of Inorganic Compounds* (Eds.: D. M. Roundhill, J. P. Fackler Jr.), Plenum Press, New York, **1999**, pp. 29–54.
- [3] M. A. Baldo, M. E. Thompson, S. R. Forrest, *Pure Appl. Chem.* **1999**, *71*, 2095.
- [4] Q. Zhang, Q. Zhou, Y. Cheng, L. Wang, D. Ma, X. Jing, F. Wang, *Adv. Mater.* **2004**, *16*, 432.
- [5] C. Fave, T. Y. Cho, M. Hissler, C. W. Chen, T. Y. Luh, C. C. Wu, R. Reau, *J. Am. Chem. Soc.* **2003**, *125*, 9254.
- [6] Y. G. Ma, C. M. Che, H. Y. Chao, X. M. Zhou, W. H. Chan, J. C. Shen, *Adv. Mater.* **1999**, *11*, 852.
- [7] Y. G. Ma, X. M. Zhou, J. C. Shen, H. Y. Chao, C. M. Che, *Appl. Phys. Lett.* **1999**, *7*, 1361.
- [8] Y. G. Ma, W. H. Chan, X. M. Zhou, C. M. Che, *New J. Chem.* **1999**, *23*, 263.
- [9] J. C. Vickery, M. M. Olmstead, E. Y. Fung, A. L. Balch, *Angew. Chem.* **1997**, *109*, 1227; *Angew. Chem. Int. Ed. Engl.* **1997**, *36*, 1179.
- [10] M. A. Mansour, W. B. Connick, R. J. Lachicotte, H. J. Gysling, R. Eisenberg, *J. Am. Chem. Soc.* **1998**, *120*, 1329.
- [11] E. Y. Fun, M. M. Olmstead, J. C. Vickery, A. L. Balch, *Coord. Chem. Rev.* **1998**, *171*, 151.
- [12] E. J. Fernández, J. M. López de Luzuriaga, M. Monge, M. E. Olmos, J. Pérez, A. Laguna, A. A. Mohamed, J. P. Fackler Jr., *J. Am. Chem. Soc.* **2003**, *125*, 2022.
- [13] Gold, *Progress in Chemistry, Biochemistry and Technology* (Ed.: H. Schmidbaur), Wiley, Chichester (UK), **1999**.
- [14] M. C. Gimeno, A. Laguna in *Comprehensive Coordination Chemistry II*, vol. 5 (Eds.: J. A. McCleverty, T. J. Meyer), Elsevier, New York, **2003**, p. 911.
- [15] P. Pykkö, *Angew. Chem.* **2004**, *116*, 4512; *Angew. Chem. Int. Ed.* **2004**, *43*, 4412.
- [16] See, for example: a) F. Canales, M. C. Gimeno, P. G. Jones, A. Laguna, *Angew. Chem.* **1994**, *106*, 811; *Angew. Chem. Int. Ed. Engl.* **1994**, *33*, 769; b) F. Canales, M. C. Gimeno, A. Laguna, P. G. Jones, *J. Am. Chem. Soc.* **1996**, *118*, 4839; c) S. Canales, O. Crespo, M. C. Gimeno, P. G. Jones, A. Laguna, *Chem. Commun.* **1999**, 679; d) S. Canales, O. Crespo, M. C. Gimeno, P. G. Jones, A. Laguna, F. Menndizabal, *Organometallics* **2000**, *19*, 4985.
- [17] a) F. Canales, M. C. Gimeno, A. Laguna, P. G. Jones, *Organometallics* **1996**, *15*, 3412; b) M. J. Calhorda, F. Canales, M. C. Gimeno, J. Jiménez, P. G. Jones, A. Laguna, L. F. Veiro, *Organometallics* **1997**, *16*, 3837; c) S. Canales, O. Crespo, M. C. Gimeno, P. G. Jones, A. Laguna, F. Mendizabal, *Organometallics* **2001**, *20*, 4812.
- [18] a) V. W. W. Yam, E. C. C. Cheng, *Gold Bull.* **2001**, *34*, 20; b) V. W. W. Yam, E. C. C. Cheng, K. K. Cheung, *Angew. Chem.* **1999**, *111*, 193; *Angew. Chem. Int. Ed.* **1999**, *38*, 197; c) V. W. W. Yam, E. C. C. Cheng, N. Zhu, *Angew. Chem.* **2001**, *113*, 1813; *Angew. Chem. Int. Ed.* **2001**, *40*, 1763; d) V. W. W. Yam, E. C. C. Cheng, *Angew. Chem.* **2000**, *112*, 4410; *Angew. Chem. Int. Ed.* **2000**, *39*, 4240; e) V. W. W. Yam, E. C. C. Cheng, Z. Y. Zhou, *Angew.*

- Chem.* **2000**, *112*, 1749; *Angew. Chem. Int. Ed.* **2000**, *39*, 1683; f) S. Lebedkin, T. Langetepe, P. Sevillano, D. Fenske, M. M. Kappes, *J. Phys. Chem. B* **2002**, *106*, 9019.
- [19] H. Shan, P. R. Sharp, *Angew. Chem.* **1996**, *108*, 811; *Angew. Chem. Int. Ed. Engl.* **1996**, *35*, 635.
- [20] H. Shan, A. James, P. R. Sharp, *Inorg. Chem.* **1998**, *37*, 5727.
- [21] A. Singh, P. R. Sharp, *Dalton Trans.* **2005**, 2080.
- [22] A. Sladek, H. Schmidbaur, *Z. Naturforsch., Teil B* **1997**, *52*, 301.
- [23] J. Olkowska-Oetzel, P. Sevillano, A. Eichhöfer, D. Fenske, *Eur. J. Inorg. Chem.* **2004**, 1100.
- [24] Q. M. Wang, Y. A. Lee, O. Crespo, J. Deaton, C. Tang, H. J. Gysling, M. C. Gimeno, C. Larraz, M. D. Villacampa, A. Laguna, R. Eisenberg, *J. Am. Chem. Soc.* **2004**, *126*, 9488.
- [25] See for example: a) A. N. Nesmeyanov, E. G. Perevalova, Y. T. Struchkov, M. Y. Antipin, K. I. Grandberg, V. P. Dyachenko, *J. Organomet. Chem.* **1980**, *201*, 343; b) A. Kolb, P. Bissinger, H. Schmidbaur, *Z. Anorg. Allg. Chem.* **1993**, *619*, 1580; c) H. Schmidbaur, A. Kolb, E. Zeller, A. Schier, H. Beruda, *Z. Anorg. Allg. Chem.* **1993**, *619*, 1575.
- [26] a) K. Angermaier, H. Schmidbaur, *Inorg. Chem.* **1994**, *33*, 2069; b) Y. Yang, V. Ramamoorthy, P. R. Sharp, *Inorg. Chem.* **1993**, *32*, 1946; c) V. Ramamoorthy, Z. Wu, Y. Yi, P. R. Sharp, *J. Am. Chem. Soc.* **1992**, *114*, 1526; d) U. M. Tripathi, A. Schier, H. Schmidbaur, *Z. Naturforsch., Teil B* **1998**, *53*, 171.
- [27] a) C. Lensch, P. G. Jones, G. M. Sheldrick, C. Thöne, *Z. Naturforsch., Teil B* **1982**, *37*, 944; b) D. Fenske, T. Langetepe, M. K. Kappes, O. Hampe, P. Weis, *Angew. Chem.* **2000**, *112*, 1925; *Angew. Chem. Int. Ed.* **2000**, *39*, 1857; c) P. Sevillano, T. Langetepe, D. Fenske, *Z. Anorg. Allg. Chem.* **2003**, *629*, 207.
- [28] E. J. Fernández, A. Laguna, J. M. López de Luzuriaga, M. Monge, M. Montiel, E. Olmos, *Inorg. Chem.* **2005**, *44*, 1163.
- [29] L. Hao, M. A. Mansour, R. J. Lachicotte, H. J. Gysling, R. Eisenberg, *Inorg. Chem.* **2000**, *39*, 5520.
- [30] V. W. W. Yam, K. L. Yu, E. C. C. Cheng, P. K. Y. Yeung, K. K. Cheung, N. Zhu, *Chem. Eur. J.* **2002**, *8*, 4122.
- [31] G. K. Patra, I. Goldberg, *Eur. J. Inorg. Chem.* **2003**, 969.
- [32] V. W. W. Yam, K. K. W. Lo, W. K. M. Fung, C. R. Wang, *Coord. Chem. Rev.* **1998**, *171*, 17.
- [33] R. P. Feazell, C. E. Carson, K. K. Klausmeyer, *Eur. J. Inorg. Chem.* **2005**, 3287.
- [34] DATAMAX 2.20, Jobin Yvon, Inc., Edison, NJ, **2001**.
- [35] Origin 5.0, Microcal Software, Inc., Northampton, MA, **1991**.
- [36] J. A. Casares, P. Espinet, K. Soulantica, I. Pascual, A. G. Orpen, *Inorg. Chem.* **1997**, *36*, 5251.
- [37] N. W. Alcock, P. Moore, P. A. Lampe, K. F. Mok, *J. Chem. Soc. Dalton Trans.* **1982**, 207.
- [38] G. J. Kubas, *Inorg. Synth.* **1979**, *19*, 90.
- [39] R. Usón, A. Laguna, M. Laguna, *Inorg. Synth.* **1989**, *26*, 85.
- [40] F. Canales, M. C. Gimeno, A. Laguna, M. D. Villacampa, *Inorg. Chim. Acta* **1996**, *244*, 95.
- [41] Bruker SADABS (Version 2.03), Bruker AXS, Inc., Madison, WI, **2000**.
- [42] SHELXL-97, A program for Crystal Structure Refinement, G. M. Sheldrick, University of Göttingen, **1997**.

Received: April 21, 2006

Published online: September 29, 2006